RESEARCH ARTICLE OPEN ACCESS

Performance Evaluation of a Pilot Solar-Powered Direct Contact Membrane Distillation Unit

Mohamad-Anas A. Hejazi*, Mohammad H. Al-Beirutty**, Omar A. Bamaga***
**Department of Mechanical Engineering, King Abdulaziz University, Saudi Arabia*
***Center of Excellence in Desalination Technology, King Abdulaziz University, Saudi Arabia*
****Center of Excellence in Desalination Technology, King Abdulaziz University, Saudi Arabia*
CorrespondingAuthor :Mohamad-Anas A. Hejazi, E-mail address: hijazipc@gmail.com

ABSTRACT
Solar-powered membrane distillation (SP MD) is a promising technology in the water desalination field. In this paper, the performance of a pilot SP MD unit located at King Abdulaziz University (KAU), Saudi Arabia was evaluated under different operating parameters during April and July 2018. A thermal analysis showed low process efficiency due to the direct contact MD configuration used. The best energy performance obtained during this study was presented in specific thermal energy consumption and gained output ratio values of 1737 kWh/m^3 and 0.37, respectively. Very high energy consumption was found at the startup of the daily operation (up to 4949.2 kWh/m^3). Operating the unit for seawater desalination gave a maximum daily averaged permeate flux of 3.36 l/m^{2}h observed during July 14 operation for a total incident solar energy of 3.996 kWh/m^2. Very high salt removal (>99.9 %) was reported in all days of operation.

Keywords-Direct contact membrane distillation, Hollow fiber module,Solar energy, Thermal energy efficiency

Date of Submission: 09-08-2018 Date of acceptance: 24-08-2018

I. INTRODUCTION

The rapid growth of population and industrial activities worldwide haveresulted in increasing the global demand for fresh water. Unfortunately, this increase inwater demand has coincided with shortages in the potable water and low rainfall rates in many areas around the world, especially in the Middle East and North Africa region. According to the world health organization, 2.1 billion people already lack the access to safe drinking water, and by 2025, half of the world population will be living in water-stressed areas [1,2].

Desalination of brackish and seawater has been presented in many countries as a solution for the shortages in the natural freshwater resources. Many of the technologies used in desalination have reached a mature level and been employed in large-scale plants worldwide since 1957 [3]. However, the desalination processes are known for their intensive energy consumption and their reliance on the conventional unsustainable energy sources like petroleum. Many countries that suffer from water scarcity do not have access to such energy sources. Even those that have these sources may face depletion in their reserves in the future [4–6], in addition to the current environmental and health issues related to the harmful combustion emissions. Fortunately, since most of the countries suffering from potable water deficits enjoy high solar isolation over the year, solar energy has the superiority over other sustainable alternatives to drive the desalination processes. Many researches have focused on incorporating solar energy with current desalination techniques like multi stage flash (MSF), multi effect (MED), and reverse osmosis (RO) [7–16].

Beside current desalination methods, an increasing research interest has been devoted to a hybrid process that combines between the thermal and membrane separation processes. Membrane distillation (MD) is a thermally-driven membrane process where only vapor molecules are transported through the pores of a microporous hydrophobic membrane. The membrane in this technology acts as a barrier to the saline solution, resulting in a liquid-vapor interface at the entrance of each pore [17]. Water vapor can pass through the pores and is condensed on the other side of the membrane [18]. The driving force of the vapor diffusion in MD is the vapor pressure difference across the membrane interfaces resulted from the temperature gradient between the two sides of it. Different configurations are used to create the vapor pressure gradient required to drive the MD process: mainly, direct contact MD, air gap MD, sweeping gas MD, and vacuum MD [19,20]. However, the attention toward DCMD has been greater than other configurations due to its simplicity and suitability for water-based applications[21,22]. Both hot feed and the condensing liquid are directly in contact with the membrane surfaces in this configuration.

Some unique advantages in MD have allowed this technology to compete with other separation processes, which include high salt rejection factor, low operating temperatures, and low operating pressures [17,23]. The low operating temperatures, typically within the range of 50 - 90 °C [24], has made MD integrable with alternative energy sources such as solar, geothermal, and waste heat energy sources. Another remarkable feature of MD is its ability to deal with highly saline solutions. This interesting feature with the low temperature requirements has allowed MD to be employed in desalinating brines coming out from MSF and RO plants, which can help in improving their water recovery ratio.

II. SP MD systems - state of the art

Many research efforts have been reported to employ solar energy for powering MD. In 1991, Hogan et al. [25] studied an SP MD system that had 3 m^2 flat plate solar collectors for production of 50L per day. This attempt was considered as the first in coupling flat plate solar collectors with MD. Their results showed the feasibility of SP MD for domestic drinking water in remote areas.

A compact SP MD unit was used by Koschikowski et al. [26] to test a new spiral wound MD module developed at Fraunhofer ISE, Germany. This module had an AGMD configuration with an effective area of 8 m^2 and internal heat recovery feature. Utilizing 5.9 m^2 solar thermal collection and connecting the electrical to the grid, the investigations showed that the permeate flux increased with the module hot inlet temperature. A maximum permeate production of 15 l/h was obtained, and the total permeate produced was 130 l/day.

Further five compact SP MD units have been installed by Fraunhofer ISE in Alexandria (Egypt), Irbid (Jordan), Pozo Izquuierdo (Grand Canary), Kelaa de Sraghna (Morroco), and Tenerinfe (Spain) [29]. Each of these systems had a 500 L feed storage, solar thermal collectors, an MD module, a pump, and a photovoltaic panel. The performance reported from these systems varied depending on the amount of solar radiation they received. Fath et al. [27–29] reported on the compact SP MD unit installed in Alexandria, Egypt. This unit also had flat plate solar collectors with an area of 6 m^2 and MD module of 7 m^2 area. The feed was brackish water. This daily unit production was 11.2 l/d while the cumulated solar energy was 41.6 kWh/d. The lowest permeate conductivity observed was 3 µS/cm. The compact SP MD unit installed in Irbid, Jordan was reported on by Banat et al. [30]. This system had flat plate solar collectors with an area of 6 m^2. The MD module had an effective area of 10 m^2 and used to desalt brackish water. The maximum permeate production was 120 l/d. The lowest permeate conductivity observed was 5 µS/cm.

In most large SP MD units, the loop of desalination is separated from the solar collector loop via a heat exchanger to protect the solar collectors from the corrosive saline feed. Also, these units usually incorporate thermal storage and batteries to extend the operating period. Several large research SP MD units have been installed around the world. Results of a largeunit installed in Aqaba, Jordan have been reported by Banat et al. [24]. This unit had 72 m^2 flat plate collectors with 3 m^3 thermal storage. Four MD modules connected in parallel have been used for real seawater desalination, each with an effective area of 10 m^2. This unit had the ability to operate for 6 hours after sunset with production ranged from 2 to 11 l/d per unit collector area and specific energy consumption in the range of 200–300 kWh/m^3.

Koschikowski et al. [29,31]studied a large SP MD unit installed in Gran Canaria. This unit had a 90 m^2 flat plate collectors, a 4 m^3 thermal storage tank, and PV panels. Five AGMD modules of 10 m^2 each were connected in parallel used to desalt seawater. The extended operation until 4:30 am gave a daily production of 1200 L.

Wang et al. [32] tested a compact SP VMD system in Hanzaghou, China. This system had 8 m^2 solar collectors and a hollow fiber module of 0.09 m^2effective area. Electrical equipment was connected to the grid. A constant vacuum of 0.9 bar was applied on the permeate side to create the vapor pressure difference. The feed used was groundwater with a conductivity of 230 mS/cm. The results showed a permeate flux as high as 32.19 l/m^2h achieved with the 8 m^2 solar energy collector. The largest daily production reported was 173.5 l/m^2 with a conductivity as low as 4 µS/cm.

A static solar field facility located at Plataforma Solar de Almería, Spain has been used by Guillén-Burrieza et al. [33] to investigate the performance of two precommercial AGMD modules. This facility had 500 m^2 compound parabolic collectors. Both modules tested had flat sheet membranes of the same type with total membrane area of 9 m^2 each. The first one was a single compact module, while the other consisted of three modules of 3 m^2 connected in series. The feed used were NaCl solutions of 1 and 35 g/ L concentration. The minimum specific thermal energy consumption (STEC) reported were 1805 kWh/m^3 for the compact module and 294 kWh/m^3 for the multi-stage one. The production and heat recovery were higher for the multi-stage module. The maximum permeate fluxes reported were 3.23 and 5.09 l/m^2h for the multi-stage and compact modules respectively. The permeate conductivity was in the range of 2–5 µS/cm.

Schwantes et al. [34] reported on two autonomous SP MD units developed by Fraunhofer ISE and installed in Namibia and Gran Canaria. The Namibia unit had 232 m^2 of flat plate solar collectors, 13 m^3 thermal storage, and 12 MD modules with a total area of 168 m^2. The treated feed in this unit was brackish water 28 g/l. The reported permeate production was 2079 l/d with an average permeate conductivity of 850 µS/cm from 1280 kWh of solar irradiation. While, the Gran Canaria unit had 186 m^2 of flat plate solar collectors, 7.2 m^3 thermal storage, and 12 MD module with a total area of 120 m^2. The feed used was seawater of 35 g/l salinity. Distillate production of 1416 l/day was reported at an average of 78 µS/cm out of 1232 kWh solar irradiation.

Kim et al. [35] investigated the performance of a large SP DCMD plant with a heat recovery arrangement for 24 h/day continuous operation. This plant had evacuated-tube solar collectors with a surface area of 3360 m^2 and 160 m^3 seawater storage. Fifty hollow fiber MD modules were used. This system produced 31 m^3/day of distillate. The system's STEC was 436 kWh/m^3 when heat recovery was used. The study found that the module dimensions, especially fiber length, was the most affecting factor on the flux. Also, it was shown that the STEC decreases significantly by increasing the solar collector area.

Shim et al. [36] investigated the desalination of seawater by SP DCMD unit in Korea. The effective area of the solar collectors was 4.7m^2, and the area of the membrane was 0.06 m^2. A long-term study of 150 days was carried out. During the daytime, more than 77.3 % of the heating energy s delivered by solar energy. The results showed a small reduction in the permeate flux from 28.48 to 26.50 l/m^2h at the end of the study.

Performance of an SP DCMD system located at KAU, Jeddah, Saudi Arabia was investigated by Bouguecha et al. [37]. This system had 20 m^2 flat plate solar collectors with 300 L thermal storage. Three hollow-fiber modules were used, each of an area of 1.4 m^2. A heat exchanger was employed for heat recovery from the permeate to preheat the feed before entering the MD modules. The effects of different operating parameters were assessed. The study also showed the benefit of recovering energy from permeate. The distillate per module was found to be 3.31 l/h without heat recovery, and it was 4.59 l/h with heat recovery.

The objective of this study is to make a contribution in this field, by evaluating the performance of a pilot-scale solar-powered (SP) DCMD unit under different operating factors and different types of saline feed water. This work covers the productivity and energy efficiency of this unit.

III. MATERIAL AND METHODS

A solar energy-powered DCMD pilot unit located at the Center of Excellence in Desalination Technology (CEDT), KAU was operated under the actual weather conditions of Jeddah, Saudi Arabia. The unitis fully equipped with the necessary instrumentation for monitoring and control of the various operating parameters in real time. The effects of operating parameters on its productivity were investigated. These parameters include the feed flow rate, feed temperature, and feed concentration. Also, a thermal analysis was done to determine the specific thermal energy consumption of the process.

3.1Experimental setup

A schematic diagram of the DCMD pilot plant is shown in Fig. 1. This unit consists of four loops: Loop (I) is the solar energy-collecting loop, to provide the thermal energy needed for heating the feed and operating the plant; Loop (II) is the photovoltaic panels loop, to provide the required electric energy; Loop (III) is the desalination loop with a hollow fiber DCMD module for fresh water production; and Loop (IV) is a 500 L capacity thermal sink, in which cold water is used to stabilize the permeate temperature for DCMD operation.

3.1.1 Solar collector loop

The solar thermalloop has eight flat plate collectors with a totaleffective area of 20 m^2. The collectors are arranged in a series: parallel (4:2) configuration. The solar collector loop is connected to the desalination loop via a heat exchanger (16 kW) to protect the solar collectors from the exposure to the saline feed water.

3.1.2 Photovoltaic panels (PV)

The PV loop consists of eight PV panels, electric batteries, and a DC/AC inverter. The eight PV panels are assembled in parallel with a peak generating capacity of 1.480 kW_{peak}. This loop is used to drive electrical equipment and the instrumentation of the plant. Two electric batteries (24 V, 100 Ah) are used to stabilize and regulate the power from the PV panels. The direct current (DC) from the batteries is converted to alternating current (AC) by a DC/AC electric inverter.

3.1.3 Membrane module

A hollow fiber membrane module of shell-and-tube configuration was used. This module is manufacturedby(Microdyn-NadirGmbH,Germany). The feed is circulated through the shell side, while the permeate in the tube side, in a counter-current mode. The vapor released from the hot feed would diffuse through the pores of the hydrophobic membranes to condense in the colder permeate stream. The technical specifications of this module are given in Table 1.

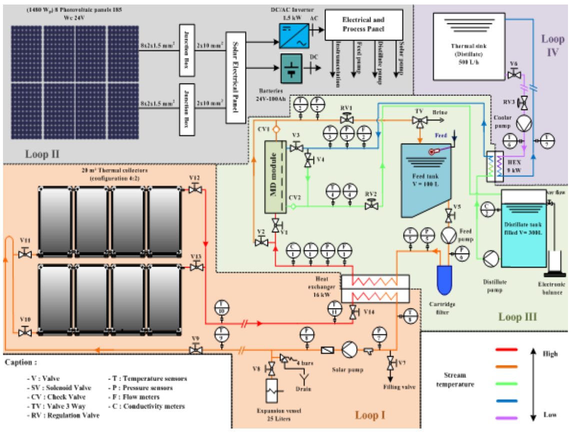

Fig. 1 Schematic diagram of the pilot DCMD unit

3.1.4 Thermal sink loop

A vapor compression chilled-water unit with a cold-water tank of 500 L capacity is used as the thermal sink for the DCMD pilot plant. This loop is connected to the permeate circulation in the desalination loop via a heat exchanger (9 kW) to absorb the heat gained by the permeate and keep its temperature at stable level; therefore, maintaining high MD driving force.

Table 1 Specifications of the module used on the pilot unit

Module model	**MICRODYN® MD 063 CP 2N**
Membrane material	Polypropylene
Module configuration	Shell-and-tube
Number of fibers	200
Fibers inner diameter (mm)	1.8
Pore size (µm)	0.2
Membrane area (m^2)	0.75

3.2Measurements and control

The plant is equipped with the necessary instrumentation for monitoring the different operating parameters. An inductive conductivity meter (Negele ILM3) is mounted on the feed line to measure the salinity of the feed stream. Another conductivity meter (Thermo Scientific Orion 3 star, USA) was used to measure the TDS of the permeate inside the permeate tank. The feed flow rate is measured using an electromagnetic flow meter (Bürkert, type 8045) fitted into the feed line. While, a paddle-wheel flow meter (Bürkert, type 8035) is fitted into the permeate line to measure the permeate flow rate. Four pressure transmitters (Cerabar PMP131 by Endress + Hauser) are installed to monitor the pressures of the MD module, one at the inlet and another at the exit of each flow line. A series of temperature sensors (thermometer TEC 420 by Endress + Hauser) are installed at various locations of the DCMD pilot plant (see Fig. 1). A pyranometer (Kipp&Zonen, type CMP3) is installed at the collector location to measure the solar radiation. An electronic balance (Tor-Rey Electronics, model LEQ 5/10) is used to measure the product overflowed from the permeate tank. This balance was connected to a PC for monitoring the yield variationsduring the operation period. A data acquisition system (Fluke Corporation, type 2635A Hydra Series II) is used to simultaneously monitor and record the signals received from all other instrumentation. The feed and permeate flow rates are adjusted by two frequency inverters (Moeller, type dv51) that control the pumps speed. In addition, two regulating valves are installed, one each at the feed and permeate exits of the MD module for adjusting the feed and permeate pressure.

3.3Experimental Procedure

The performance was investigated by operating the pilot unit for several days during April 2018 under the variable solar thermal input. The operation was during the daylight hours without controlling the feed temperature, while the inlet permeate temperature to the MD module was fixed at 23 ±1 ºC. The permeate flow rate was fixed at 600 l/h, while different feed flow rates were used to study the effect of the feed flow rate on the performance. In addition, the effect of the feed salinity was investigated using three different types of feed: tap water, pre-treated seawater, and seawater RO (SWRO) brine with TDS values of 85, 36720, and 55390 mg/l, respectively. The operating conditions during April operation are presented in Table 2.

The performance of this unit was evaluatedin terms of the permeate flux, the salt rejection, and the specific thermal energy consumption of the MD module. The permeate flux was calculated from the permeate tank overflow using the following equation:

Table 2 Daily operating conditions during April 2018

	Type of feed water	Feedflowrate [l/h]	Permeate flowrate [l/h]	Feed temperature [°C]	Permeatetemperature [°C]
April 16	Tap water	600	600	Variable with the solar radiation	23±1
April 17	Tap water	800			
April 18	Tap water	1000			
April 19	Seawater	800			
April 22	SWRO brine	800			

$$J = \frac{W}{t*A} \quad (1)$$

Where W is the overflowed permeate weight in kg; t is the time in hours, and A is the membrane module effective area in m^2.The salt rejection which describes the percentage of salt removal from the water stream is given by

$$SR = \frac{C_f - C_p}{C_f} \times 100 \quad (2)$$

Where C_f and C_p are the concentrations of the feed and permeate, respectively in ppm.

The specific thermal energy consumption (STEC) is one of the importantcharacteristics of thermal seawater-desalination plants which represents the heat required for producing a specific amount of distilled water [30]. The STEC (kWh/m^3) of the MD module is defined as the ratio of thermal energy supplied to the module to the volume of distillate produced and it is given by

$$STEC = \frac{Q_{in}}{\dot{m}_d} \quad (3)$$

Where Q_{in} is MD module power input in kW, and $\dot{m}_d$ is the distillate yield flow rate in m^3/h. Q_{in} is given by the following simple thermodynamic equation

$$Q_{in} = \dot{m}_h C_p \left(T_{h,i} - T_{h,o}\right) \quad (4)$$

Where $\dot{m}_h$ is the feed flow rate in kg/h, C_p is the specific heat of the feed solution at constant pressure in kj/kg.K, $T_{h,i}$ and $T_{h,o}$ are the module feed inlet and outlet temperatures, respectively in K.

Another important parameter normally used to assess the efficiency of thermal desalination processes is the gained output ratio (GOR). The GOR is defined as the energy ratio of the latent heat of evaporation of the product water to the module input thermal energy [26] which is given by

$$GOR = \frac{\dot{m}_d h_{fg}}{Q_{in}} \quad (5)$$

Whereh_{fg} is the water latent heat of vaporization in kj/kg, and $\dot{m}_d$ here is in kg/h.The latent heat of vaporization is influenced by the salinity and extremely by temperature [38]. So, firstly, the h_{fg} of the pure water at the different operating temperatureis calculated using the following correlation (obtained by fitting the data of the water h_{fg}[39] to a second-order polynomial)

$$h_{fg} = 2497.6 - 2.1044\,T - 0.0031T^2 \quad (6)$$

Where$T$ in ^{0} C, and the correlation R² = 0.9998 for water temperatures in the range of 0 – 180 ^{0} C. Then, the h_{fg} of the saline water is calculated by the following equation [38]

$$h_{fg,sw} = h_{fg} \times \left(1 - \frac{S}{1000}\right) \quad (7)$$

Finally, the pilot unit was operated for several daysduring July 2018 for desalting seawater. The daily averaged permeate flux and salt removal were reported with the incident solar energy.

IV. RESULTS AND DISCUSSION

Fig. 2 shows the operation graphs of the pilot MD unit during April. These graphs present the solar radiation, the module temperatures profile, and the permeate flux of the MD module during operation. The starting and the shutdown times are also presented for each day on the time axis of each graph. Table 3 gives information about the daily maximum and average values of the solar radiation and feed temperatures in addition to the permeate flux obtained during operation. The highest permeate flux of 4.3 L/m^{2}h was recorded during April 17 at a feed inlet temperature of 67 ºC. The effects of the feed temperature, feed salinity, and the feed flow rate on the unit productivity and efficiency are discussed in the sub-sections 4.1 to 4.4.

Table 3 Daily performance of the pilot MD unit within study duration

	April 16	***April 17***	***April 18***	***April 19***	***April 22***
Avg. solar radiation [W/m^2]	857.63	873.60	809.53	816.11	819.75
Max. solar radiation [W/m^2]	970.00	989.04	931.69	939.40	961.81
Avg. feed temperature [ºC]	61.80	60.63	57.22	59.96	60.65
Max. feed temperature [ºC]	67.71	67.03	62.72	65.84	65.80
Avg. permeate flux [l/m^{2}h]	3.12	3.40	3.10	2.95	2.90
Max. permeate flux [l/m^{2}h]	4.29	4.30	3.72	3.73	3.31

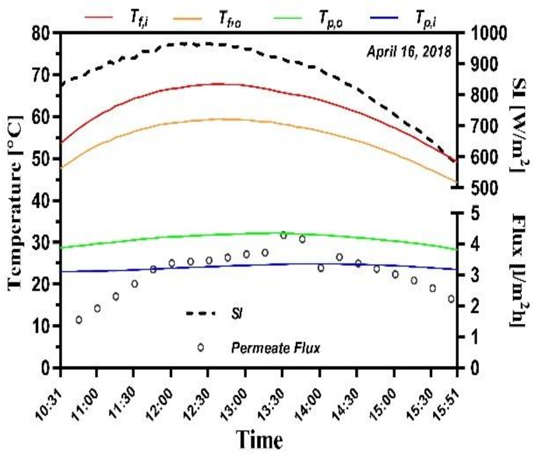

(a)

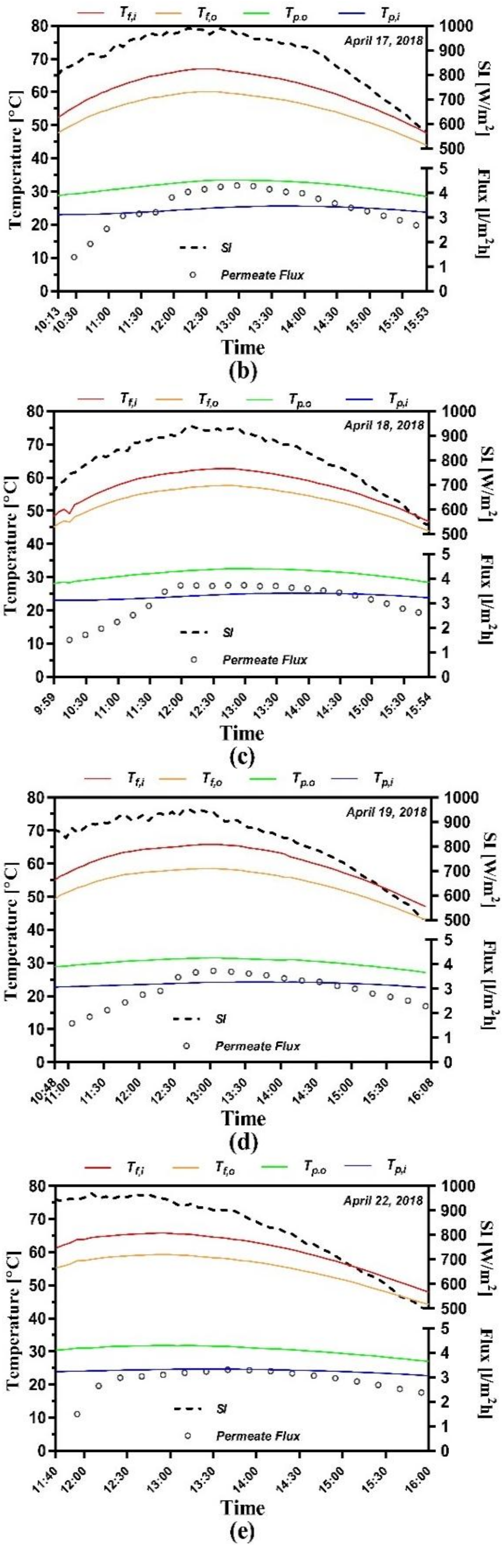

Fig. 2 Daily operation profiles during the pilot MD April experiments

4.1Effect of feed temperature

Fig. 3 shows the permeate flux as a function of the feed temperature for three different feed flow rates, while the permeate temperature, as well as the permeate flow rate, were maintained constant at 23 ±1 ºC and 600 l/h, respectively. Increasing the feed temperature leads to higher permeate fluxes. For example, at a feed flow rate of 800 l/h, increasing the feed temperature from 57 to 67 ºC increased the permeate flux by 121%.

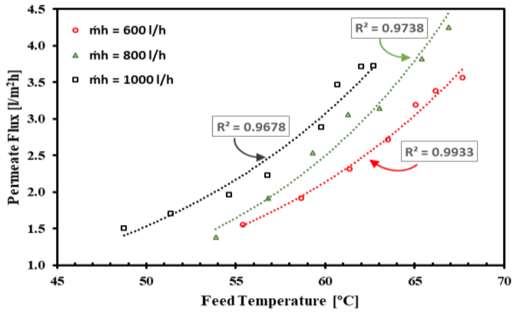

Fig. 3 Effect of feed temperature on the permeate flux of the pilot MD unit; Where $T_{c,i}$ =23 ±1 ºC and $\dot{m}_c$=600 l/h.

Also, the curves in Fig. 3 show an exponential relationship between the permeate flux and the feed temperature. That was attributed to the exponential relationship between the vapor pressure and temperature from the Antoine equation [40,41].

4.2Effect of feed flow rate

Fig. 4 shows the performance of the MD module in terms of the permeate flux against the feed flow rate at three different feed temperatures. The experimental results showed that the feed flow rate has a significant effect on the permeate flux and this effect increases for higher feed temperatures. For example, at 57 ºC, increasing the feed flow rate from 600 to 1000 l/h leads to 35.8 % increase in the permeate flux, while, at 62 ºC, the same increase in the feed flow rate results in 47.1% increase in permeate flux. The productivity enhancement is attributed to the higher Reynolds numbers (i.e., higher turbulence) that reduce the thickness of the hydrodynamic and thermal boundary layers and therefore, reducing the temperature and concentration polarization effects at the membrane interface. This increases the convective heat transfer coefficient which in turn enhances the driving force across the membrane. However, the observed relationship between the permeate flux and the feed mass flow rate is logarithmic with an asymptotic trend when the feed flow rates reach very high values. Hence, the effect of feed temperature on the productivity (exponential trend) is found to be higher than that of the feed flow rate.

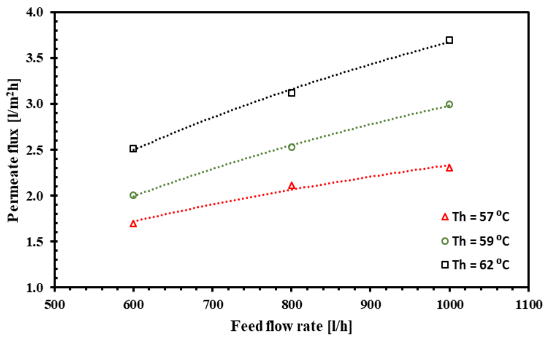

Fig. 4 Effect of feed flow rate on the permeate flux of the pilot MD unit; Where $T_{c,i}$ =23 ±1 ºC and $\dot{m}_c$=600 l/h.

4.3Effect of feed salinity

Fig. 5 shows the effect of the feed salt concentration on the module permeate flux. The permeate flux of the different feed types (tap water, seawater, and SWRO brine) is presented by their TDS values at two different feed temperatures. As can be seen, the salinity of the feed solution tends to affect the permeate flux of the membrane module negatively. For example, at a feed temperature of 65.4 ºC, the permeate flux decreased by 16.5% when SWRO brine was used as feed instead of tap water. The observed decline in flux can be attributed to a decrease in the transmembrane driving force resulted from the decrease of the vapor pressure of water with increasing salt concentration. Also, the increase in solute concentration increase the temperature and concentration polarization effects.

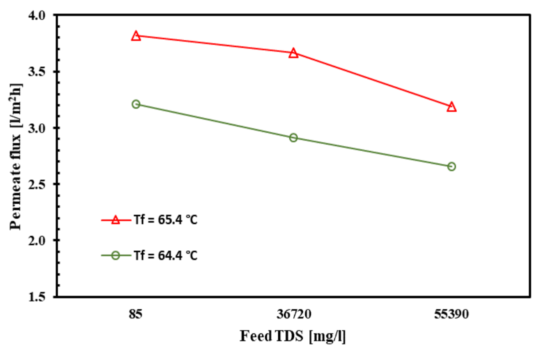

Fig. 5 Effect of feed salinity on the permeate flux of the pilot MD unit; Where $T_{c,i}$ =23 ±1 ºC, $\dot{m}_h$=800 l/h and $\dot{m}_c$=600 l/h.

4.4Energy consumption of the MD module

Fig. 6 presents the permeate flux, module power input, and the module specific thermal energy consumption profiles for the pilot unit operation on April 16, as an example. As can be seen, the initial STEC value was very high (4003.7 kWh/m^3), which is attributed to the low permeate flux at the operation startup. The STEC value was significantly decreased during the first hour of operation by the permeate flux increase and reached a minimum of 1737.1 kWh/m^3 at 01:46 pm. During the last two hours of operation, both permeate flux and power input decreased, but the resultant was a slight increase in the STEC.

The taken data during the days of study allowed to investigate the effect of the operating parameters on the process efficiency. Fig. 7 shows the effect of feed flow rate on the energy consumption and the GOR of the module at two different feed temperatures. The results obtained shows that increasing the feed flow rate, in the range of the flow rates used in this study (600-1000 l/h), leads to increasing the GOR and decreasing the energy consumption of the module. For example, at a feed temperature of 62.4ºC, increasing the feed flow rate from 600 to 1000 L/h results in rising the GOR from 0.219 to 0.302 and lowering the STEC from 2986.7 to 2164.2 kWh/m^3. These results show the positive effect of the feed flow rate on the process efficiency. However, the MD studies reported by other researches showed that the performance increases with increasing the feed flow rate to some limit; after that, the GOR and the STEC tend to decrease, which suggests optimum values for the feed flow rate [36,42–44].

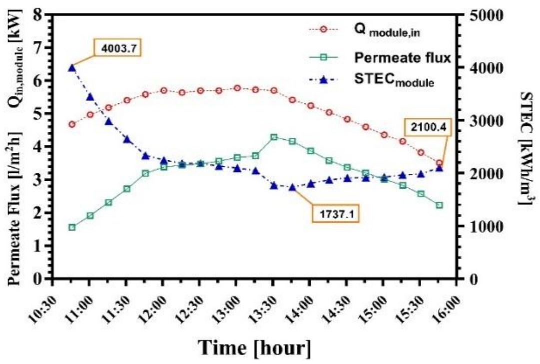

Fig. 6 STEC profile during operation.

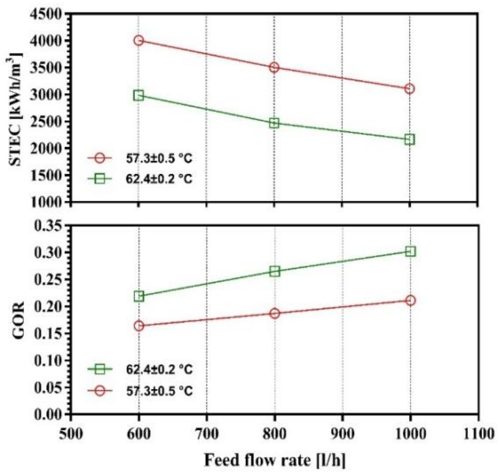

Fig. 7 Effect of feed flow rate on the STEC & GOR of the pilot MD unit; Where $T_{c,i}$ =23 ±1 ºC and $\dot{m}_c$=600 l/h.

The effect of feed salinity on the GOR and the STEC is shown in Fig. 8. As can be seen, the higher feed salinity, the higher the STEC. For instance, at a feed temperature of 65.4 ºC, using SWRO brine as a feed instead of tap water lowered the GOR from 0.30 to 0.24 and increased the STEC from 2172.3 to 2599.7 kWh/m^3. Therefore, the salinity of the feed solution is seemed to affect the efficiency of the MD process negatively.

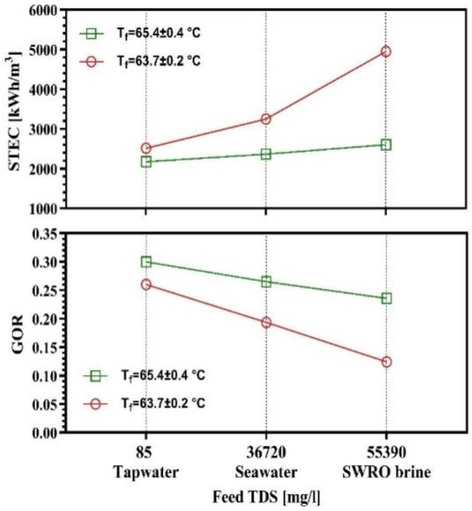

Fig. 8 Effect of feed salinity on the STEC & GOR of the pilot MD unit; Where $T_{c,i}$ =23 ±1 ºC,$\dot{m}_h$=800 l/h and $\dot{m}_c$=600 l/h.

Moreover, the effect of feed temperature can be seen inFig. 7 and Fig. 8. The higher the feed temperature the high GOR and the lower STEC. The positive effect of feed temperature was observed at any feed salinity or flow rate.

Overall, the values of the STEC and the GOR during operation ranged from 1737.1- 4949.2 kWh/m^3 and from 0.12- 0.37, respectively. These values indicate low performance and high energy consumption MD process and attributed to the low permeability of the used module. The low efficiency is widely reported in the DCMD systems (STEC values ranged from 600 to 4580 kWh/m^3 [45–47]). In contrast, the reported results from AGMD systems show higher performance due to the lower conductive heat losses in these systems [24,26,31]. Khayet in his review [48] described a wide range of dispersion in the energy consumption of MD systems reported in the literature (very wide range from about 1 to 9000 kWh/m^3). The author mentioned some of the factors that led to this dispersion, which include: the lack of optimization in the MD systems design, the absence of a standard for the calculations of MD performance, the differences in the operating conditions, the system scale, and other factors related to the fouling and long-term operation.

4.5 The unit performance during July

The unit was operated for seawater desalination during several days during July 2018 with a daily operating period of five hours. Over this period, the daily incident solar energy in kWh/m^2 of collector area, the avg. permeate flux in l/h per module area and the salt removal in percentage are presented in Fig. 9.

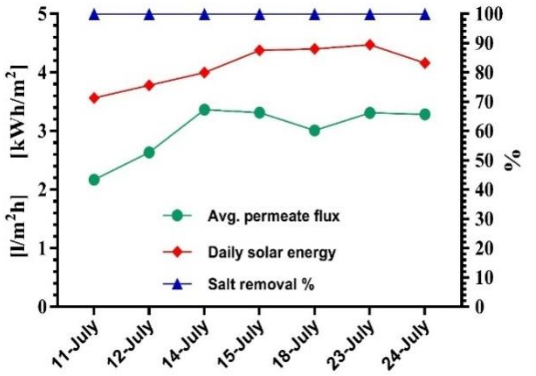

Fig. 9 Operation during July 2018; Where $T_{c,i}$ =25 ±1 ºC,$\dot{m}_h$=900 l/h and $\dot{m}_c$=600 l/h.

The highest daily avg. permeate flux of 3.36 l/m^{2}h was observed during July 14 operation with a total incident solar energy of 3.996 kWh/m^2. In the next days, the permeate flux was slightly lower even when the solar radiation was higher. Thisis attributed to higher wind speeds during these days, which was confirmed from the records of King Abdulaziz International Airport weather station (MID OEJN), Jeddah, SA. The higher wind speed results in higher energy losses through the long connecting pipes in the solar loop. On the other hand, very high salt removal was observed during all days of operation (up to 99.996%).

V. CONCLUSIONS

Set of experiments was conducted during April 2018 to evaluate the performance of the SP DCMD pilot plant located at CEDT- KAU, under the actual weather conditions of Jeddah, Saudi Arabia. The plant performance was evaluated as a function of the operating parameters. The feed temperature was found to significantly enhance the permeate flux of the MD module in an exponential trend. At a feed flow rate of 800 l/h, increasing the feed temperature from 57 to 67 ºC led to 121% increase in the permeate flux. The feed flow rate was also seen to affect the permeate production of the MD module positively but in logarithmic trend. The use of different types of feed water in the pilot unit allowed to investigate the effect of salinity on the permeate production. It was found that feed salinity affects the productivity of MD negatively. At a feed temperature of 65.4 ºC, using SWRO brine as feed instead of tap water resulted in a 16.5% decline in the permeate flux.

Thermal analysis for the module of the pilot unit, in terms of the STEC and the GOR, showed the low efficiency of the DCMD process compared to other reported AGMD pilot systems. The best energy performance obtained during this study was presented in STEC and GOR values of 1737 kWh/m^3 and 0.37, respectively. During all days of study, high initial energy consumption values were observed during the first hour of operation (up to 4949.2 kWh/m^3), which were attributed to the low permeate flux during the startup period. The low efficiency is attributed to the module low permeation characteristics.

The effect of the studied parameters on the unit efficiency was also investigated. The high feed temperatures resulted in more efficient MD process. Also, within the range of flow rates used in this study, the feed flow rate was found to affect the process efficiency positively. In contrast, using high salinity feed water resulted in lower MD efficiency seen in the high STEC and low GOR values.

Finally, the unit was operated for seawater desalination during July 2018. A maximum daily avg. permeate flux of 3.36 l/m^{2}h was observed during July 14 operation at a total incident solar energy of 3.996 kWh/m^2. High salt removal (>99.9 %) was reported in all days of operation.

Nomenclature

A	membrane area (m^2)
C	concentration (ppm)
C_p	specific heat (kJ/kg.K)
h_{fg}	latent heat of vaporization (kJ/kg)
J	permeate flux (l/m^{2}h)
$\dot{m}$	flow rate (kg/h)
Q	power (W)
SR	salt rejection (%)
T	temperature (K)
t	time (h)
W	weight (kg)

Subscripts

f	feed
h	hot
p	permeate
c	cold
d	distillate
i	inlet
o	outlet
in	input
sw	seawater

REFERENCES

[1]. Drinking-water, World Heal. Organ. (2018). http://www.who.int/news-room/fact-sheets/detail/drinking-water (accessed July 9, 2018).

[2]. Progress on drinking water, sanitation and hygiene: 2017 update and SDG baselines, 2017. http://www.who.int/water_sanitation_health/publications/jmp-2017/en/.

[3]. K.V. Reddy, N. Ghaffour, Overview of the cost of desalinated water and costing methodologies, Desalination. 205 (2007) 340–353. doi:10.1016/J.DESAL.2006.03.558.

[4]. R.L. Hirsch, Mitigation of maximum world oil production: Shortage scenarios, Energy Policy.36(2008)881889.doi:10.1016/J.ENPOL.2007.11.009.

[5]. D.J. Murphy, C.A.S. Hall, Adjusting the economy to the new energy realities of the second half of the age of oil, Ecol. Modell. 223(2011)6771.doi:10.1016/J.ECOLMODEL.2011.06.022.

[6]. J.H. Brown, W.R. Burnside, A.D. Davidson, J.P. DeLong, W.C. Dunn, M.J. Hamilton, N. Mercado-Silva, J.C. Nekola, J.G. Okie, W.H. Woodruff, W. Zuo, Energetic Limits to Economic Growth, Bioscience. 61 (2011) 19–26. doi:10.1525/bio.2011.61.1.7.

[7]. D.-C. Alarcón-Padilla, L. García-Rodríguez, Application of absorption heat pumps to multi-effect distillation: a case study of solar desalination, Desalination. 212 (2007) 294–302. doi:10.1016/J.DESAL.2006.10.014.

[8]. A.N.A. Mabrouk, H.E.S. Fath, Experimental study of high-performance hybrid NF-MSF desalination pilot test unit driven by renewable energy, Desalin. Water Treat. 51 (2013)68956904.doi:10.1080/19443994.2013.773860.

[9]. L. García-Rodríguez, Renewable energy applications in desalination: State of the art, Sol. Energy. 75 (2003) 381–393. doi:10.1016/j.solener.2003.08.005.

[10]. A.M. Delgado-Torres, L. García-Rodríguez, Comparison of solar technologies for driving a desalination system by means of an organic Rankine cycle, Desalination. 216 (2007) 276–291. doi:10.1016/J.DESAL.2006.12.013.

[11]. L. García-Rodríguez, A.M. Delgado-Torres, Solar-powered Rankine cycles for fresh water production, Desalination. 212 (2007) 319–327. doi:10.1016/J.DESAL.2006.10.016.

[12]. A.M. Delgado-Torres, L. García-Rodríguez, Status of solar thermal-driven reverse osmosis desalination, Desalination. 216 (2007) 242–251. doi:10.1016/J.DESAL.2006.12.014.

[13]. A.B. Pouyfaucon, L. García-Rodríguez, Solar thermal-powered desalination: A viable solution for a potential market, Desalination. 435(2018)6069.doi:10.1016/J.DESAL.2017.1

2.025.

[14]. M. Thomson, D. Infield, A photovoltaic-powered seawater reverse-osmosis system without batteries, Desalination. 153 (2003) 1–8. doi:10.1016/S0011-9164(03)80004-8.

[15]. B. Peñate, J.A. de la Fuente, M. Barreto, Operation of the RO Kinetic® energy recovery system: Description and real experiences, Desalination. 252 (2010) 179–185. doi:10.1016/j.desal.2009.06.078.

[16]. L. García-Rodríguez, Seawater desalination driven by renewable energies: a review, Desalination. 143 (2002) 103–113. doi:10.1016/S0011-9164(02)00232-1.

[17]. K.W. Lawson, D.R. Lloyd, Membrane distillation, J. Memb. Sci. 124 (1997) 1–25. doi:10.1016/S0376-7388(96)00236-0.

[18]. M.S. El-Bourawi, Z. Ding, R. Ma, M. Khayet, A framework for better understanding membrane distillation separation process, J. Memb. Sci. 285 (2006) 4–29. doi:10.1016/j.memsci.2006.08.002.

[19]. A. Alkhudhiri, N. Darwish, N. Hilal, Membrane distillation: A comprehensive review, Desalination. 287 (2012) 2–18. doi:10.1016/j.desal.2011.08.027.

[20]. B.B. Ashoor, S. Mansour, A. Giwa, V. Dufour, S.W. Hasan, Principles and applications of direct contact membrane distillation (DCMD): A comprehensive review, Desalination. 398 (2016) 222–246. doi:10.1016/j.desal.2016.07.043.

[21]. M. Khayet, Membranes and theoretical modeling of membrane distillation: A review, Adv. Colloid Interface Sci. 164 (2011) 56–88. doi:10.1016/J.CIS.2010.09.005.

[22]. Y. Yun, R. Ma, W. Zhang, A.G. Fane, J. Li, Direct contact membrane distillation mechanism for high concentration NaCl solutions, Desalination. 188 (2006) 251–262. doi:10.1016/j.desal.2005.04.123.

[23]. H. Susanto, Towards practical implementations of membrane distillation, Chem. Eng. Process. Process Intensif. 50 (2011) 139–150. doi:10.1016/J.CEP.2010.12.008.

[24]. F. Banat, N. Jwaied, M. Rommel, J. Koschikowski, M. Wieghaus, Performance evaluation of the “large SMADES” autonomous desalination solar-driven membrane distillation plant in Aqaba, Jordan, Desalination. 217 (2007) 17–28. doi:10.1016/j.desal.2006.11.027.

[25]. P.A. Hogan, Sudjito, A.G. Fane, G.L. Morrison, Desalination by solar heated membrane distillation, Desalination. 81 (1991) 81–90. doi:10.1016/0011-9164(91)85047-X.

[26]. J. Koschikowski, M. Wieghaus, M. Rommel, Solar thermal driven desalination plants based on membrane distillation, Desalination. 156 (2003) 295–304. doi:10.1016/S0011-9164(03)00360-6.

[27]. H.E.S. Fath, S.M. Elsherbiny, A.A. Hassan, M. Rommel, M. Wieghaus, J. Koschikowski, M. Vatansever, PV and thermally driven small-scale, stand-alone solar desalination systems with very low maintenance needs, Desalination. 225 (2008) 58–69. doi:10.1016/J.DESAL.2006.11.029.

[28]. H.E.S. Fath, S.M. A.Elsherbiny, A. Hassan, M. Rommel, M. Wieghaus, J. Koschikowski, M. Vatansever, PV and thermally driven small-scale, stand-alone solar desalination system, in: IDA World Congr. Gran Canar., Elsevier, 2007: pp. 21–26. doi:10.1016/J.DESAL.2006.11.029.

[29]. R.B. Saffarini, E.K. Summers, H.A. Arafat, J.H. Lienhard V, Technical evaluation of stand-alone solar powered membrane distillation systems, Desalination. 286 (2012) 332–341. doi:10.1016/j.desal.2011.11.044.

[30]. F. Banat, N. Jwaied, M. Rommel, J. Koschikowski, M. Wieghaus, Desalination by a “compact SMADES” autonomous solarpowered membrane distillation unit, Desalination. 217 (2007) 29–37. doi:10.1016/j.desal.2006.11.028.

[31]. J. Koschikowski, M. Wieghaus, M. Rommel, V.S. Ortin, B.P. Suarez, J.R. Betancort Rodríguez, Experimental investigations on solar driven stand-alone membrane distillation systems for remote areas, Desalination. 248 (2009) 125–131. doi:10.1016/J.DESAL.2008.05.047.

[32]. X. Wang, L. Zhang, H. Yang, H. Chen, Feasibility research of potable water production via solar-heated hollow fiber membrane distillation system, Desalination. 247(2009)403411.doi:10.1016/J.DESAL.2008.10.008.

[33]. E. Guillén-Burrieza, G. Zaragoza, S. Miralles-Cuevas, J. Blanco, Experimental evaluation of two pilot-scale membrane distillation modules used for solar desalination, J. Memb. Sci. 409410(2012)264275.doi:10.1016/j.memsci.2012.03.063.

[34]. R. Schwantes, A. Cipollina, F. Gross, J. Koschikowski, D. Pfeifle, M. Rolletschek, V. Subiela, Membrane distillation: Solar and waste heat driven demonstration plants for desalination, Desalination. 323 (2013) 93–106. doi:10.1016/j.desal.2013.04.011.

[35]. Y.D. Kim, K. Thu, N. Ghaffour, K. Choon Ng, Performance investigation of a solar-assisted direct contact membrane distillation

system, J. Memb. Sci. 427 (2013) 345–364. doi:10.1016/j.memsci.2012.10.008.

[36]. W.G. Shim, K. He, S. Gray, I.S. Moon, Solar energy assisted direct contact membrane distillation (DCMD) process for seawater desalination, Sep. Purif. Technol. 143 (2015) 94–104. doi:10.1016/J.SEPPUR.2015.01.028.

[37]. S.T. Bouguecha, S.E. Aly, M.H. Al-Beirutty, M.M. Hamdi, A. Boubakri, Solar driven DCMD: Performance evaluation and thermal energy efficiency, Chem. Eng. Res. Des. 100 (2015)331340.doi:10.1016/j.cherd.2015.05.044.

[38]. M.H. Sharqawy, J.H. Lienhard, S.M. Zubair, Thermophysical properties of seawater: a review of existing correlations and data, Desalin. Water Treat. 16 (2010) 354–380. doi:10.5004/dwt.2010.1079.

[39]. C. Borgnakke, R.E. Sonntag, Fundamentals of Thermodynamics, 8th ed., Wiley, 2013.

[40]. F.A. Banat, J. Simandl, Theoretical and experimental study in membrane distillation, Desalination. 95 (1994) 39–52. doi:10.1016/0011-9164(94)00005-0.

[41]. A.M. Alklaibi, N. Lior, Membrane-distillation desalination: Status and potential, Desalination. 171 (2005) 111–131. doi:10.1016/J.DESAL.2004.03.024.

[42]. E. Ali, J. Orfi, A. Najib, Assessing the Thermal Efficiency of Brackish Water Desalination by Membrane Distillation Using Exergy Analysis, Arab. J. Sci. Eng. (2017). doi:10.1007/s13369-017-2831-5.

[43]. N. Palanisami, K. He, I.S. Moon, Utilization of solar energy for direct contact membrane distillation process: An experimental study for desalination of real seawater, Korean J. Chem. Eng. 31 (2014) 155–161. doi:10.1007/s11814-013-0250-1.

[44]. S. Al-Obaidani, E. Curcio, F. Macedonio, G. Di Profio, H. Al-Hinai, E. Drioli, Potential of membrane distillation in seawater desalination: Thermal efficiency, sensitivity study and cost estimation, J. Memb. Sci. 323 (2008)8598.doi:10.1016/j.memsci.2008.06.006.

[45]. M. Khayet, J.I. Mengual, G. Zakrzewska-Trznadel, Direct contact membrane distillation for nuclear desalination, Part II: experiments with radioactive solutions, Int. J. Nucl. Desalin. 2 (2006) 56. doi:10.1504/IJND.2006.009505.

[46]. G. Zakrzewska-Trznadel, M. Harasimowicz, A.G. Chmielewski, Concentration of radioactive components in liquid low-level radioactive waste by membrane distillation, J. Memb. Sci. 163 (1999) 257–264. doi:10.1016/S0376-7388(99)00171-4.

[47]. M.C. Carnevale, Evaluation of energy requirements in membrane distillation, Chem. Eng. Process. Process Intensif. 47 (2008) 1098–1105. doi:10.1016/J.CEP.2007.03.006.

[48]. M. Khayet, Solar desalination by membrane distillation: Dispersion in energy consumption analysis and water production costs (a review), Desalination. 308 (2013) 89–101. doi:10.1016/j.desal.2012.07.010.

Mohamad-Anas A. Hejazi"Performance Evaluation of a Pilot Solar-Powered Direct Contact Membrane Distillation Unit "International Journal of Engineering Research and Applications (IJERA) , vol. 8, no.8, 2018, pp 51-61